

# IRREGULAR ATMOSPHERIC EFFECTS ON SATELLITE OBSERVATIONS

K. LAMBECK

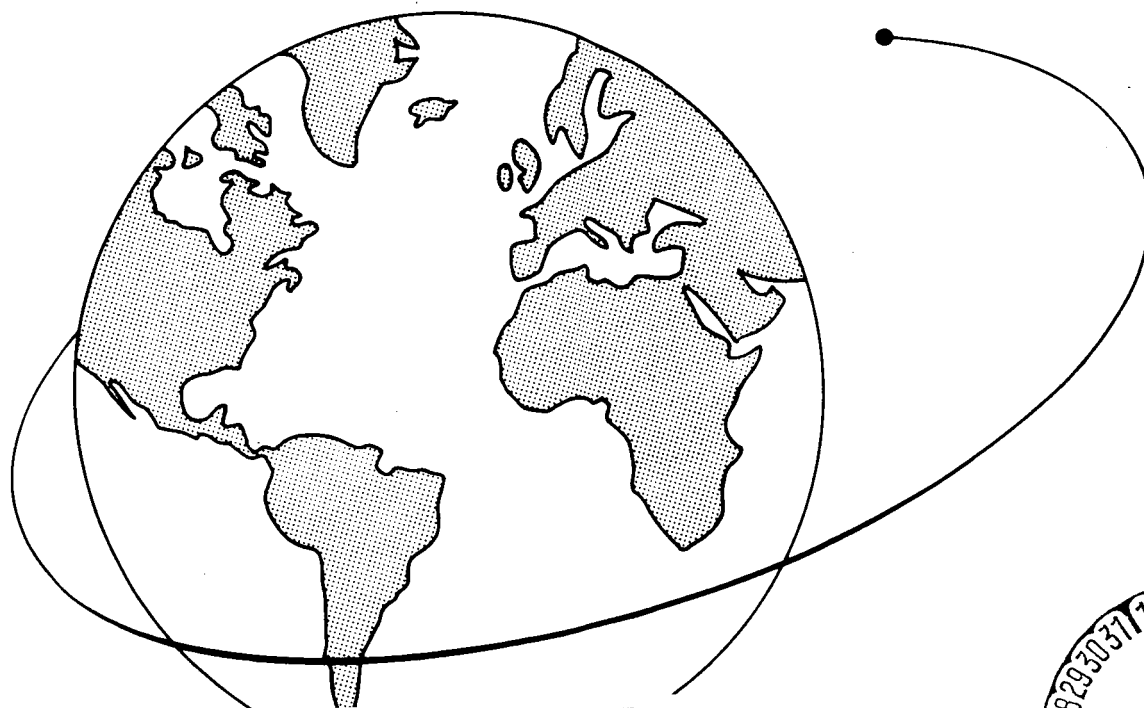
GPO PRICE \$ \_\_\_\_\_

CFSTI PRICE(S) \$ \_\_\_\_\_

Hard copy (HC) 3.00

Microfiche (MF) .65

ff 653 July 65



FACILITY FORM 602

N 68-29706 (THRU) \_\_\_\_\_

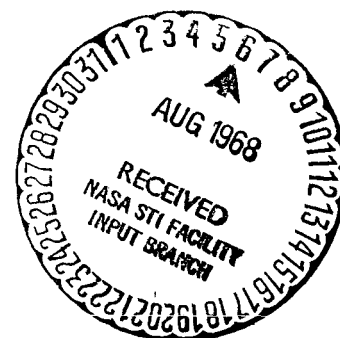
(ACCESSION NUMBER)

34 (PAGES) \_\_\_\_\_

(CODE) \_\_\_\_\_

CR-95809 (NASA CR OR TMX OR AD NUMBER) \_\_\_\_\_

(CATEGORY) \_\_\_\_\_



Smithsonian Astrophysical Observatory  
SPECIAL REPORT 269

Research in Space Science  
SAO Special Report No. 269

EFFECT OF RANDOM ATMOSPHERIC REFRACTION  
ON OPTICAL SATELLITE OBSERVATIONS

K. Lambeck

March 15, 1968

Smithsonian Institution  
Astrophysical Observatory  
Cambridge, Massachusetts 02138

TABLE OF CONTENTS

<u>Section</u>		<u>Page</u>
	ABSTRACT. . . . .	iv
1	INTRODUCTION . . . . .	1
2	GENERAL DISCUSSION ON IMAGE MOTION . . . . .	2
3	MATHEMATICAL FORMULATION OF THE IMAGE MOTION. . . . .	6
4	OBSERVATIONAL DATA . . . . .	11
5	ATMOSPHERIC-TURBULENCE CHARACTERISTICS . . . . .	20
6	CONCLUSIONS . . . . .	22
	REFERENCES . . . . .	25

## LIST OF ILLUSTRATIONS

<u>Figure</u>		<u>Page</u>
1	Results of image motion as a function of aperture . . . . .	11
2	Relationship between image motion (reduced for aperture and zenith distance) and exposure time, based on data presented in Table 3. . . . .	17
3	Average one-dimensional image motion as a function of aperture and exposure time for observations in the zenith. .	18
4	Possible method for observing image motion . . . . .	24

## LIST OF TABLES

<u>Table</u>		<u>Page</u>
1	Results of image-motion measurements by <u>Hansson et al.</u> (1950) reduced to the zenith according to $\sec z$ and $\sec^{1/2} z$ . . . . .	13
2	Summary of image-motion observations from various investigators. . . . .	14
3	Results of slow-period image-motion observations . . . . .	15
4	Temperature and refractive index fluctuations as a function of wind velocity required to explain the image motion. . . .	21

## ABSTRACT

A study is made of the effects on optical satellite observations of image motion resulting from microturbulence in the troposphere. A formulation, based on theoretical and heuristic considerations as well as on limited observational data, enables the magnitude of the image motion to be estimated as a function of lens aperture, exposure time, and zenith distance.

## RÉSUMÉ

Une étude est faite des effets sur les observations optiques de satellites du mouvement de l'image résultant de la micro-turbulence dans la troposphère. Une formulation basée autant sur des considérations théoriques et heuristiques que sur un nombre limité de données expérimentales permet d'estimer l'ordre de grandeur du mouvement de l'image en fonction de l'ouverture de l'objectif, du temps d'exposition et de la distance zénithale.

## КОНСПЕКТ

Производится изучение влияний движения изображения происходящего в результате микротурбулентности в тропосфере на оптические наблюдения спутников. Формулировка, основанная на теоретических и исследовательских соображениях а также и на ограниченных данных наблюдений, позволяет оценку величины движения изображения как функции апертуры линзы, времени экспозиции и зенитного расстояния.

# EFFECT OF RANDOM ATMOSPHERIC REFRACTION ON OPTICAL SATELLITE OBSERVATIONS

K. Lambeck

## 1. INTRODUCTION

An electromagnetic wave traversing the atmosphere will undergo several changes, of which the bending of the ray path and the change in velocity of the wave are of greatest importance for satellite tracking. Extinction and polarization also occur, but these are generally of lesser importance. For precise observations, the variations in the velocity and curvature of the ray path cannot be ignored, and these effects on the observed quantities must be estimated, usually by an approximation of the physical atmosphere by mathematical models.

The perturbations from the ideal vacuum conditions are caused by the departure of the refractive index of the earth's atmosphere from unity and by the variability of this index with both space and time. These departures and variations are partly systematic; they can be predicted and the observed quantities corrected to varying degrees of reliability. But random variations from these predictions remain and are often at least as important as the systematic parts. At optical frequencies, the distinction is quite clear and the two can be treated independently; the systematic parts are inferred when the terms optical, astronomical, or parallactic refraction and absorption are used, and the random parts are usually referred to as scintillation, seeing, or image motion. The former can be adequately predicted by use of simple models that are a function of space and only indirectly of time, while the latter tend to defy such descriptions and are probably best treated by statistical methods; it is this aspect of atmospheric refraction that will be considered here.

---

This work was supported in part by Grant NsG 87-60 from the National Aeronautics and Space Administration.

## 2. GENERAL DISCUSSION ON IMAGE MOTION

A distant object, when viewed through a telescope, will appear to "dance" about a mean position as well as to exhibit fluctuations in intensity. The former phenomenon is usually referred to as image motion and the latter as scintillation, although the terminology used in the literature is often varied and confusing. Some authors use scintillation to refer to all the erratic behavior characteristics of the image, whereas in the strict sense, it refers to the rapid intensity fluctuations only and is independent of the size or motion of the image. Scintillation, therefore, does not influence the accuracy of spatial position determination to nearly the same extent as the actual image motion or dancing does.

The term seeing describes the image characteristics, referring to the continually changing position, shape, and size of the image, but again some authors include in its meaning pulsation, focus drift, and scintillation as well. This confusion is all the more important when it is realized that there appears to be little correlation between many of the different phenomena.

In this paper, only the effect of image motion on the precision of direction observations of extraterrestrial objects and, more specifically, artificial earth satellites will be discussed. A detailed study of scintillation is given by Nettleblad (1953), and a useful literature survey of scintillation and image motion is given by Meyer-Arendt and Emmanuel (1965).

Image motion arises from atmospheric turbulences, which produce random fluctuations in the refractivity. Consequently, the ray path deviates randomly and continuously from its mean position. The motion is irregular in both amplitude and frequency, but observations of the phenomena indicate that there are two broad categories into which the periods fall: those with a slow oscillatory motion, and those with a high frequency.

The different periods of the motion are essentially a function of the size of the irregular air masses or "blobs" intercepting the ray path. The long-period fluctuations or "wandering" are due to large air masses, perhaps of the order of 50 m, while the rapid motions have their origin in air masses of sizes down to about 10 cm.

Schlesinger (1916) and Hudson (1929) have indicated that the wandering has a period of about 1 min and deviates from the mean position by about 0.5 arcsec. More recent observations by Land (1954) verify these orders of magnitude.

The rapid image motion, or dancing, has periods very much shorter than a second of time and amplitudes up to several seconds of arc (see for example, Hansson, Kristensen, Nettleblad, and Reiz, 1950; Hosfield, 1954). Little seems to be known about these high frequencies, apart from the fact that they do exist. But more observational evidence is available for the short-period intensity fluctuations, and although there is little evidence to suggest that there is any correlation between image motion and scintillation, it is feasible that the periods and amplitudes of the two phenomena behave in similar patterns; namely, that (Nettleblad, 1953)

1. The frequencies reach values up to some hundred cycles per second and the most rapid variations are of smaller amplitudes.
2. The observed frequencies and amplitudes decrease with increasing aperture.
3. The period and amplitude also increase with increasing zenith distance.

Refraction anomalies exist in all regions of the atmosphere, but certain areas may be of greater importance than others. Menzel (1962) distinguishes three regions that may be of significance. The first is the turbulence of the air in the telescope itself. Differences in internal and external temperatures may give rise to complicated patterns of convection inside the telescope and may result in deterioration of the image. The simplest way to suppress these eddies, at least partially, is to allow the instrument to "acclimatize"



before the commencement of observation and to allow the air to circulate freely through it. This should ensure as nearly a uniform temperature as possible, both internally and externally to the telescope. More sophisticated ways are to evacuate the telescope tube of all gas or to replace the air by a gas of lower refractive index, such as helium, but these methods have obvious disadvantages for cameras used in satellite tracking.

The second source of atmospheric turbulence lies in the air layers immediately outside the objective lens. The camera housing, the instrument itself, or the surrounding ground and vegetation may possess different heat capacities than does the surrounding air, and consequently, they may act as heat sources or sinks. Partial remedies are the removal of the camera housing from the instrument during observations and the positioning of the camera away from likely sources of temperature anomalies, as well as at some distance above the ground. Results quoted by Meyer-Arendt and Emmanuel (1965) indicate that an elevation of the instrument to about 7 to 10 m above the ground level is desirable.

The third zone is in the higher atmosphere, from about 100 m upward. Turbulence in this region cannot be controlled in the way it can be in the other two regions, but it would appear that this third zone is of lesser importance than the others, partly owing to the fact that the size of the air masses will tend to increase with increasing height and partly because the refractive power of the atmosphere decreases rapidly with increasing elevation.

In optical satellite tracking, the total exposure time during which the satellite is observed against the star background is often considerably less than a minute, and slow period fluctuations will affect the satellite and star images alike, provided they lie within close proximity. When the stars lie farther apart — as may often be the case — there may be a differential displacement of the reference points. If  $n$  such points are used to determine the satellite position, the positional error introduced by the wandering would be roughly  $1/\sqrt{n}$  times the displacement of a single position. In the case of

Baker-Nunn camera observations, the exposure time of a single frame is seldom more than a few seconds, and from six to eight reference stars are used to determine the satellite position. Assuming an amplitude of 0.5 arcsec for the wandering, as suggested by Schlesinger and Hudson, the satellite positional error caused by stellar wandering would be of the order of 0.3 arcsec — an amount that at present is considerably less than the other error sources.

With ballistic cameras, the total exposure time is generally longer, owing to the necessity of taking calibration exposures before and after the passage of the satellite across the field of view. Typical calibration exposure cycles for the Wild BC-4 are of the order of 10 sec repeated six or more times. The total calibration exposure is therefore of the same order as the period of the wandering, and the image displacement will generally be averaged out when each star image in the calibration sequence is used.

Thus, while wandering would appear to have little effect on the stellar positions, it could displace the satellite trail image systematically during the short time interval that this object is in the field of view. Similarly, while the short-period deviations will generally be time averaged out for the slow-moving stellar images, displacements in the satellite image — both along track and across track — may occur because of the much faster velocity of this object.

The above and subsequent discussions make it quite clear that any formulation of the image motion must, of necessity, be based on some simplifying assumptions and that correction of individual positions for the image displacements will be impossible. However, what will be of interest is the approximate knowledge of the image-motion behavior with certain camera characteristics, particularly the aperture and exposure time, and of the orders of magnitude of the displacements that could be expected under "average" or "typical" conditions. It is on these factors that the emphasis will be placed in the following analysis.

### 3. MATHEMATICAL FORMULATION OF THE IMAGE MOTION

Various theories have been proposed to explain the erratic image characteristics. Refraction theory offers the simplest explanation; starting with irregular refractions caused by density anomalies, the ray path deviates from the normals to these blobs, according to the laws of geometric optics. As these blobs change size or position with time, so does the ray-path direction vary. Diffraction theory offers an alternate explanation: plane-wave fronts entering a turbulent medium are distorted, and adjacent parts of the wave leaving the layer will be randomly out of phase. Yet another approach, based on statistical theory, has been developed by Chandrasekhar (1952). Making the assumptions that variations in the refractive index are small and that the conditions in the disturbed layer can be approximated by those in homogeneous isotropic turbulence, Chandrasekhar derives the following expression for the standard deviation of the image motion:

$$\sigma_{\psi}^2 = 0.55 \times 10^6 \left( \frac{s}{r_0} \right)^{1/2} \sigma_n^2, \quad (1)$$

where  $s$  is the distance the ray path travels through the disturbed medium,  $r_0$  is the micro scale (that is, the size of the blobs) of the turbulence, and  $\sigma_n$  is the standard deviation of the refractive-index fluctuations. It may be desirable to express the fluctuations in refractivity as temperature variations. To a first approximation, the refractive index is given by

$$n - 1 = 109 \frac{p}{T} 10^{-6},$$

where  $n$  is the refractive index,  $p$  the pressure in mm Hg, and  $T$  in degrees absolute. Differentiation of this yields

$$dn = 109 \left( \frac{\partial p}{T} - \frac{p}{T^2} \partial T \right) 10^{-6}.$$

But from the equation of state for adiabatic processes in a perfect gas

$$\frac{p}{T} \frac{\partial T}{\partial p} = \frac{\gamma - 1}{\gamma} \quad ,$$

where  $\gamma$ , the adiabatic lapse rate, for air is equal to about 1.4. Hence,

$$dn = 109 \times 10^{-6} \frac{p}{T^2} \frac{1}{\gamma - 1} dT \quad ,$$

and for 760 mm Hg and 10° C,

$$\sigma_n = 2.6 \times 10^{-6} \sigma_T \quad .$$

The standard deviation of the image motion as a function of temperature fluctuations is, therefore,

$$\sigma'_\psi = 1.45 \left( \frac{s}{r_0} \right)^{1/2} \sigma_T \quad . \quad (2)$$

Equations (1) and (2) give the deviation of a ray path through an infinitely small aperture. If an objective of aperture  $D$  is used to form the image, a number of such rays will combine to form an average or space-integrated image whose motion will be somewhat less than that of a single ray. Assuming that the blobs of air have an average diameter of  $r_0$ , there will be  $(D/r_0)^2$  such air masses in front of the objective; assuming further that these blobs will move independently of each other — in other words, that there is no correlation between the deviations of rays passing through adjacent air masses — the image motion will be the average of  $(D/r_0)^2$  single rays. That is,

$$\sigma_\psi \propto \left( \frac{r_0^2}{D^2} \right)^{1/2} \quad . \quad (3)$$

Obviously, the relationship is valid only for  $D \geq r_0$ ; for  $D < r_0$ , the displacement will be that for a single ray.

The relationship (3) is very much simplified from what can be expected to exist in reality, for in the first place it assumes that all the blobs are of equal size, and in the second place it assumes that adjacent air masses move independently. In actual fact, there may be a whole spectrum of blob sizes or of refractivity anomalies, and their movement may follow a more or less regular pattern. A more sophisticated attempt to establish the relation between image motion and aperture would therefore be to assume a spectrum of eddy sizes that oscillate according to some pattern — for example, a sinusoidal law, as can be expected if the blobs move past the objective at a constant velocity due to wind — and to integrate over both the lens aperture and the adopted spectrum. Such an approach, however, has not been developed here, because the detailed knowledge of the properties of atmospheric turbulence required for such an analysis still appears to be lacking. The spectra of the refractive index fluctuations with time or height are as yet unavailable, and there is a shortage of reliable image-motion observations from which such information could be deduced. Furthermore, the chief interest in the study of the image motion for the astronomer and the satellite observer is to determine the magnitude of the displacement rather than to derive models for the atmospheric turbulence. For these reasons, a single blob size that moves at random in a turbulent region up to a height  $h$  will be considered, and a simple relation of the form

$$\sigma_{\psi} \propto \frac{1}{D^m} \quad , \quad m \leq 1 \quad ,$$

will be sought instead.

The relation between image motion and zenith distance  $z$  is equally obscure. The path length  $s$  is approximately related to  $z$  according to  $s = h \sec z$ , suggesting that

$$\sigma_{\psi} \propto \sec^{1/2} z \quad ,$$

but the fact that  $r_0$  may also be a function of the zenith distance will complicate the relationship, and in general, it would be expected that

$$\sigma_{\psi} \propto \sec^{n/z} , \quad n \geq 0.5 .$$

The observed image motion will also be a function of the exposure time, for if this interval is greater than the period of a particular oscillation, there will be a time integration of the resulting image. To a first approximation, this time integration can be deduced by the assumption that the air is a "frozen" layer of blobs moving past the objective at a constant velocity  $V$ . The number of blobs  $f$  passing any point in time  $\delta t$  will then be

$$f = \frac{V}{r_0} \delta t ,$$

and the resultant time-averaged image motion will be proportional to

$$\left[ \int_{\Delta T} \left( \frac{r_0}{Vt} \right) dt \right]^{1/2} = \left( \frac{r_0}{V} \right)^{1/2} (K - \ln \Delta T)^{1/2} ,$$

where  $\Delta T$  is the exposure interval in seconds and  $K$  is the integration constant. As before, the variations in the size and velocity of the air masses moving across the objective will be irregular, so that generally

$$\sigma_{\psi} \propto (K - \ln \Delta T)^p , \quad p \geq 0.5 .$$

The complete formulation of the image motion will now be of the form

$$\sigma_{\psi}'' = \frac{1.45 (r_0 h)^{1/2} \sec^{n/z} \left( \frac{r_0}{V} \right)^{1/2}}{D^m} (K - \ln \Delta T)^p \sigma_T , \quad \begin{cases} m \leq 1 \\ n \geq 0.5 \\ p \geq 0.5 \end{cases} . \quad (4)$$

A limited amount of observational evidence is available to suggest possible values for the parameters inherent in the above equation; this will be used in the following section to derive estimates of the orders of magnitude that can be expected for the image motion.

The fluctuations in the refractive index could conceivably also cause variations in range observations measured at optical frequencies using, for example, lasers.

Chandrasekhar (1952) gives the following expression for the standard deviation  $\sigma_r$  of range measurements, at optical frequencies, due to turbulence:

$$\sigma_r = 1.34 (hr_0)^{1/2} \text{ sec}^{1/2} z \sigma_n ,$$

where  $h$ ,  $r_0$ , and  $\sigma_n$  have the same meaning as before; if the former two quantities are measured in centimeters,  $\sigma_r$  will also be in centimeters.

#### 4. OBSERVATIONAL DATA

The only systematic attempt at establishing a relationship between image motion and aperture, based on actual observations, appears to have been by Rösch (1957, 1958a, 1958b). His 1958 results are given in Figure 1; they indicate that, at least between the aperture limits of 10 and 50 cm,

$$\sigma_{\psi} \propto \frac{1}{D^{1/2}} \quad (5)$$

These results also indicate that for apertures greater than about 20 cm, the relationship

$$\sigma_{\psi} \propto \frac{1}{D}$$

is almost equally valid, suggesting that air turbulences separated by about this order of magnitude are correlation free.

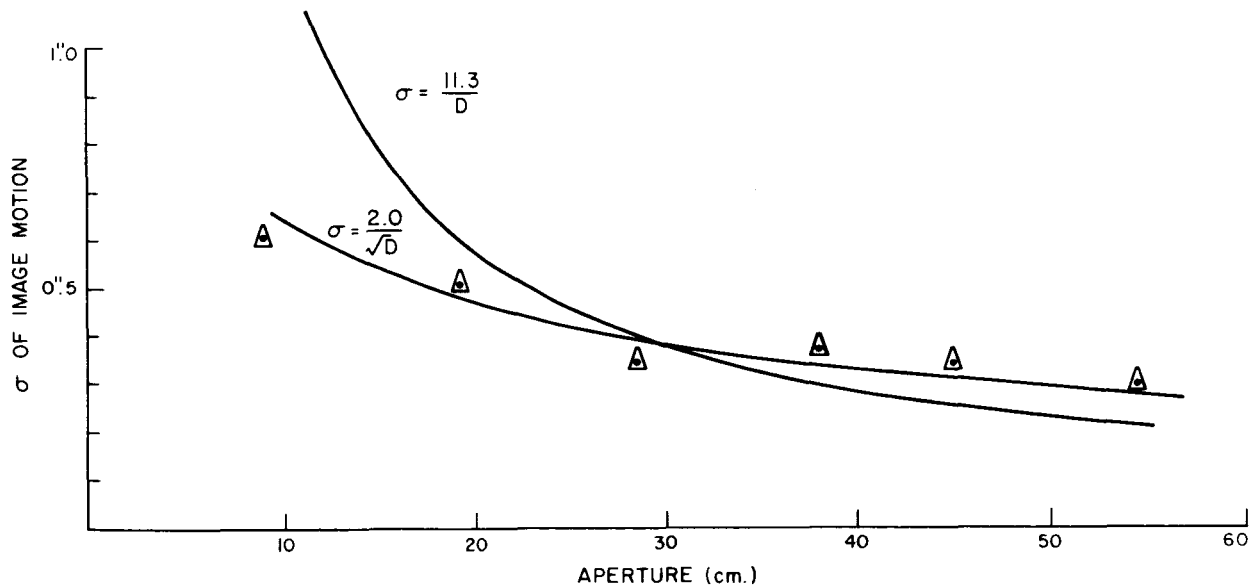


Figure 1. Results of image motion as a function of aperture. The symbols  $\Delta$  are the values observed by Rösch (1958b).



Measurements to determine experimentally the relationship between image motion and zenith distance have been made by several investigators, but the interpretation of the results is conflicting. Strömgren (Nettleblad, 1953, p. 27) indicates a  $\sec^{1/2} z$  law, while Kolchinsky (Nettleblad, 1953, p. 34) also concludes that in most cases this is so and that in no circumstances is the exponent as high as unity. Hansson et al. (1950), on the other hand, indicate a  $\sec z$  variation. Their results are presented in Table 1. However, their limited data indicate that the  $\sec^{1/2} z$  law is just as valid. Boutet (1950) found that the general law was a  $\sec z$  one, but that sometimes a proportionality to  $\sec^{1/2} z$  or to  $\sec^2 z$  existed.

Further observations of image motion have been made by Barocas and Withers (1948), Couder (1936), Hosfield (1954), and Hynek (1963). Their results, together with those of Hansson et al., Strömgren, and Rösch are listed in Table 2. All observations are for night conditions.

Barocas and Withers measured the oscillations in star trails of Talcott pairs. Measurements of stellar positions were made at 0.1-mm intervals, which correspond approximately to exposure intervals of about 0.1 sec. All observations were made near zenith, and the average deviations from the mean of each trail ranged from about 0.3 to 0.6 arcsec. The value given in Table 3 is the standard deviation of all their measurements.

Couder obtained his results by forming four images of a star onto a moving film. He achieved these images by placing a disk, containing four circular openings along a diameter, in front of the telescope lens such that the four openings were normal to the direction of the film motion. In each opening a slightly deviating prism was placed so that a star in the field of view yields four separated image trails, the relative positions of which are free of any instrument vibrations. No direct exposure time is given by Couder, but it appears that the parts of the traces measured correspond to about 0.035 sec. His results also indicated that trails formed by openings separated by 17 cm showed almost no correlation, suggesting that the blob size must be of this order or less.

Table 1. Results of image-motion measurements by Hansson et al. (1950) reduced to the zenith according to  $\sec z$  and  $\sec^{1/2} z$

$\sigma''_{\psi}$ (observed)	Sec z	$\sigma''_{\psi}$ reduced to zenith according to $\sec z$	$\sigma''_{\psi}$ reduced to zenith according to $\sec^{1/2} z$
0.50	1.09	0.46	0.47
0.52	1.15	0.45	0.49
0.53	1.16	0.46	0.49
0.53	1.18	0.45	0.48
0.53	1.21	0.44	0.48
0.56	1.12	0.50	0.53
0.59	1.16	0.51	0.55
0.60	1.23	0.49	0.54
0.63	1.16	0.54	0.58
0.60	1.50	0.40	0.49
0.61	1.55	0.39	0.49
0.63	1.75	0.36	0.48
0.68	1.77	0.38	0.51
0.69	1.70	0.41	0.53
0.71	2.20	0.32	0.48
0.76	2.15	0.35	0.52
0.72	2.40	0.30	0.46
0.80	2.50	0.32	0.51
	Mean	0.420	0.505
	Standard deviation from mean	0.07	0.03

Table 2. Summary of image-motion observations from various investigators

Event 1	Observer 2	D (cm) 3	t 4	z 5	Observed aperture 6	$\sigma$ image motion				Remarks 10
						Reduced for aperture 7	Reduced for zenith dist. 8	Reduced for exposure 9	Greenwich, duration of one night	
1	Barocas and Withers (1948)	16.5	1/10	3° to 10°	0.40	1.64	1.64	6.8	6.8	Greenwich, duration of one night
2	Hansson et al. (1950)	9.0	1/50	49	0.78	2.34	1.89	3.7	3.7	Lund, Sweden
3	Hansson et al. (1950)	9.0	1/50	40	0.67	2.01	1.75	3.5	3.5	Jävan, Sweden
4	Hansson et al. (1950)	9.0	1/50	39	0.81	2.43	2.15	4.2	4.2	Gödelöv, Sweden
5	Hansson et al. (1950)	9.0	1/50	47	0.70	2.10	1.73	3.5	3.5	Kläggoröd, Sweden
6	Strömberg (Nettleblad, 1953)	9.0	1/50	0	0.51	1.53	1.53	3.0	3.0	Copenhagen, several nights
7	Couder (1936)	10.0	1/30	0	0.43	1.36	1.36	3.2	3.2	Forcalquier, France
8	Rösch (1957)	19.0	1/25	-	0.5	2.18	-	-	-	Pic du Midi, France
9	Rösch (1957)	38.0	1/25	-	0.2	1.23	-	-	-	Pic du Midi
10	Rösch (1958b)	9.0	1/25	39	0.60	1.80	1.58	Average value 1.79	4.6	single set of observations made on the same night
	Rösch (1958b)	19.0	1/25	39	0.40	1.75	1.54			
	Rösch (1958b)	28.0	1/25	39	0.35	1.85	1.62			
	Rösch (1958b)	38.0	1/25	39	0.38	2.34	2.05			
	Rösch (1958b)	45.0	1/25	39	0.33	2.28	2.00			
	Rösch (1958b)	54.0	1/25	39	0.30	2.20	1.93			
11	Hosfield (1954)	7.6	1/25	65	1.13	3.11	2.03	5.2	5.2	Delaware, Ohio
12	Schmid (1965)	10.0	1/60	-	1.30	4.11	3.45	6.4	6.4	Average results of many plates An average zenith distance of 45° is assumed
13	Schmid (1965)	10.0	1/1000	-	1.80	5.70	4.18	4.8	4.8	
14	Hynek (1963)	7.6	1/60	-	1.50	4.30	3.62	6.7	6.7	Delaware, Ohio. Typical of several measurements. An average zenith distance of 45° is assumed
15	Abbey and Tavenner (1967)	20.0	1/1000	50	1.10	4.94	3.18	3.2	3.2	Average of many measurements at different locations

Table 3. Results of slow-period image-motion observations

Observer	Period (min)	Standard deviation of image motion (arcsec)	Aperture (inch)
Schlesinger (1916)	1	0.3	40.0
Schlesinger (1916)	1	0.3	22.0
Hudson (1929)	1	0.3	7.5
Land (1954)	1	0.3	25.0

Strömngren improved upon Couder's method by introducing a rotating shutter between the lens and the film. Hansson et al. and Hosfield used similar techniques.

Rösch obtained his results from an analysis of the edge functions given by stars as they occult a sharply defined edge. The image motion will result in a displacement of the edge function in the image space. Intensity scintillation and the spread functions of the optics will also cause deterioration of the edge function from the expected theoretical shape, but by studying different parts of this curve, Rösch has been able to isolate the various effects.

Hynek made his observations by photographing star images in the focal plane, by use of rapid-sequence photographs.

Schmid (1965) also gives results that are indicative of image motion. The characteristics of satellite motion are generally such that the orbit over a short arc can be approximated by a smooth curve. Rapid successive observations, however, made of the rapidly moving object will indicate deviations from the smooth curve, and at least part of these discrepancies can be attributed to image motion.

The standard deviation of the residuals obtained by Schmid are of the order  $3.0 \mu$  across track and  $3.5 \mu$  along track. The plate measurements contribute about  $2.0 \mu$ , and emulsion creep possibly a further micron, so that the image motion can be expected to be about 2 and  $2.7 \mu$  across and

along track, respectively. For the 300-mm lens, these values are equivalent to about 1.3 and 1.8 arcsec. It is tempting to assume that the measuring accuracy is equal in both the across- and along-track components, since the exposure intervals differ in these two directions, and provide additional information at very short exposures. The timing accuracy of consecutive breaks in the satellite trail is of the order of 40 to 60  $\mu$ sec and is considerably smaller than are the other error sources. For the across-track component, the exposure time is 1/60 sec, while that for the along-track component is less than 1 msec.

Some recent estimates of high-frequency image motions have been obtained by Abbey and Tavenner (1967) from an analysis of Geos-A flash observations. The cameras used are the PC 1000, which have an aperture of about 20 cm, and the duration of the observed flash is about 1 msec. Abbey and Tavenner's estimated average displacements of the images from their mean position due to atmospheric turbulence is of the order of 1.0 arcsec. These results must, however, be considered with caution, for not only may there be other factors that contribute in part to the total displacements, but plates that show large deviations from the mean positions are not included in their analysis.

The variety of methods used to obtain the estimates of image motion makes the results in Table 2 rather difficult to interpret, particularly when long focal-length instruments have been used. Long-focus telescopes mean that the contribution of errors in plate measurements and emulsion shifts are of lesser importance than in short-focus cameras, but they are more prone to image motion caused by turbulence inside the telescope than are the smaller instruments. Results obtained with long focal-length telescopes may therefore not necessarily be valid for short-focus cameras, and vice versa.

Columns 3, 4, and 5 of Table 2 give the aperture (in centimeters), the exposure time (in fractions of a second), and the zenith distance at which the observations have been made. Column 6 gives the observed one-dimensional image motion. The next column reduces the observed amount for the aperture

integration according to equation (5). Column 8 reduces the data to the zenith according to the  $\sec^{1/2} z$  law, and the only remaining variable is now the exposure interval. The image motion reduced for aperture and for zenith distance is plotted against exposure time  $\Delta t$  (in milliseconds) in Figure 2 and indicates an approximate logarithmic relationship according to

$$\sigma_{\psi}'' \propto (1 - 0.38 \log \Delta t) .$$

Column 9 gives the image motion reduced according to this relation; the average value of this motion is 4.5. The image motion can then be written as

$$\sigma_{\psi}'' = 4.5 (1 - 0.38 \log \Delta t) \frac{\sec^{1/2} z}{\sqrt{D}} . \quad (6)$$

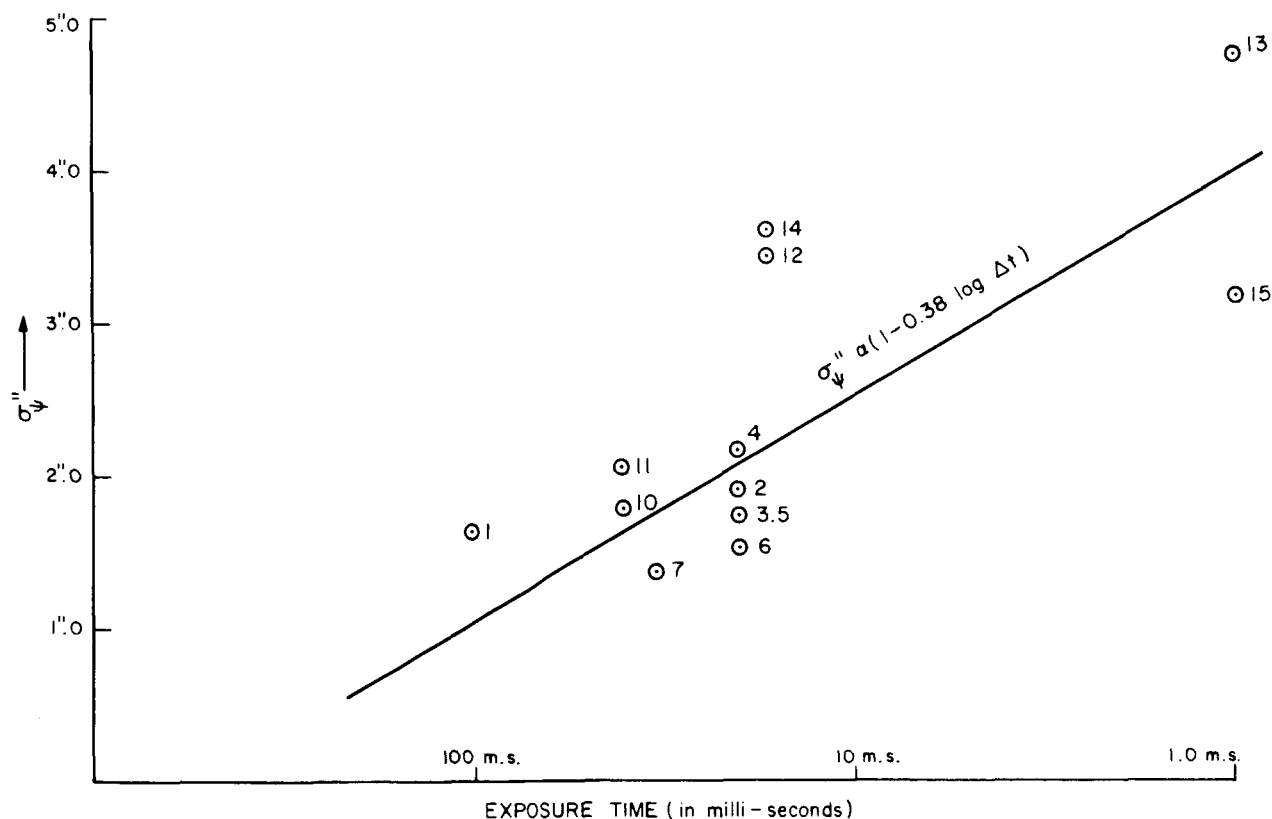


Figure 2. Relationship between image motion (reduced for aperture and zenith distance) and exposure time, based on data presented in Table 3.

Expression (6) is one-dimensional. For image motion in a two-dimensional space, this value must be multiplied by a factor of  $\sqrt{2}$ .

Obviously, because of the variety of data used in obtaining the above value of 4.5, equation (6) must be considered as being representative of "average" seeing conditions. The differences between this mean value and the various reduced values should furnish some idea of the range of the image motion. Thus, the standard deviation of  $k = 4.5$  is 1.3, or about 25% of the value of  $k$ .

Figure 3 gives  $\sigma_\psi$  as a function of exposure time  $\Delta t$  and of aperture  $D$  for observations made near the zenith.

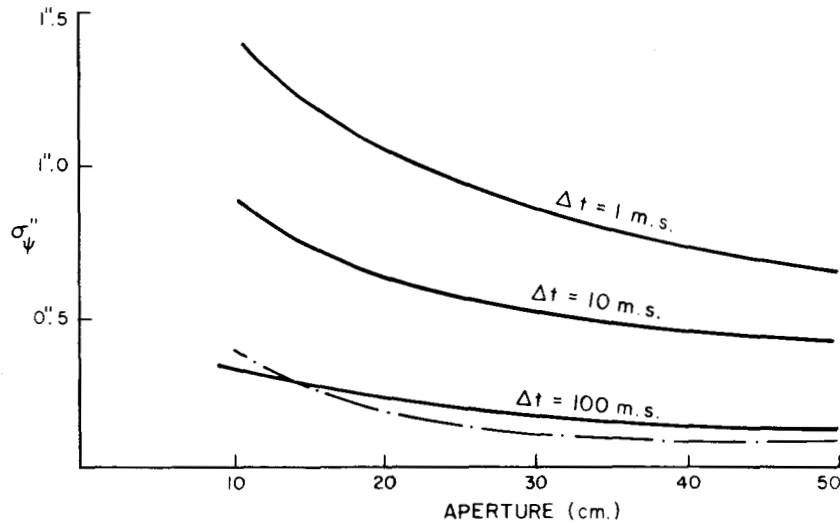


Figure 3. Average one-dimensional image motion as a function of aperture and exposure time for observations in the zenith. The broken line indicates the formulation by Brown (1960).

Observational data for the slow-period motion is given in Table 3. All investigators obtained similar results for both the period and the amplitude of the wandering, which suggested that the air masses causing the motion are larger than the largest apertures used. The studies of Schlesinger (1916), Hudson (1929), and Land (1954) also indicate that images separated by up to

a degree will appear to move in similar and simultaneous patterns. Furthermore, Hudson makes the observation that simultaneous observations to the same star from two stations separated by about 55 m will exhibit fluctuations that will have little in common.

The observations listed in Table 3 have generally been made over short time intervals, so that the observed displacements do not include the effects of wandering. The total one-dimensional image displacement, therefore, is

$$(\sigma_{\psi}^{\prime\prime})_{\text{total}} = \left\{ (0.3)^2 + \left[ 4.5 \frac{\sec^{1/2} z}{\sqrt{D}} (1 - 0.38 \log \Delta t) \right]^2 \right\}^{1/2} .$$

Equation (6) is the formulation of the image motion based on observational evidence, while equation (4) is the formulation in terms of the parameters defining the actual atmospheric turbulence. A comparison of the two will therefore make an estimate of these parameters possible and will indicate the validity of the two approaches.



## 5. ATMOSPHERIC-TURBULENCE CHARACTERISTICS

As already indicated, the results of Rösch and Couder indicate an average eddy size of about 20 cm. In equation (4) there are, however, three further parameters: the height of the turbulent layer, the velocity of the air mass moving past the objective, and the magnitude of the temperature or refractivity fluctuations. With the limited data available, it is not possible to solve for all three unknowns, and furthermore, the  $V$  and  $\sigma_T$  are not necessarily independent parameters. As is evident from the discussion above, if care is taken to reduce the air turbulence in the telescope, most of the image motion will be caused by turbulence in the first 100 m of the atmosphere.

The image-motion expression derived from the observed data can be rewritten in the form

$$\sigma_{\psi}'' = 0.74 (-0.85 - \ln \Delta T) ,$$

where  $\Delta T$  is in seconds.

Equating this expression with equation (4) yields

$$1.45 (r_0 h)^{1/2} \left(\frac{r_0}{V}\right)^{1/2} \sigma_T = 0.74$$

or

$$\frac{\sigma_T}{V^{1/2}} = \frac{0.74}{1.45 \times r_0 h^{1/2}} ,$$

and if we use the above values for  $r_0$  and  $h$ ,

$$\frac{\sigma_T}{V^{1/2}} = 2.5 \times 10^{-4} \text{ } ^\circ\text{C}/(\text{cm}/\text{sec})^{1/2} .$$

Table 4 indicates the values of  $\sigma_T$  as a function of the velocity of the air blobs past the objective that are required to satisfy the above equality. The corresponding refractive-index anomalies required are also indicated; they are of a magnitude that is reasonable to expect (see, e. g., Megaw, 1954; Chandrasekhar, 1952).

Table 4. Temperature and refractive index fluctuations as a function of wind velocity required to explain the image motion.

V (mph)	V (cm/sec)	$\sigma_T$	$\sigma_N$
1	45	0.002	$0.005 \times 10^{-6}$
5	225	0.004	$0.01 \times 10^{-6}$
10	550	0.006	$0.02 \times 10^{-6}$

The observations of Hudson (1929) enable estimates to be made of the upper limits both to the eddy size and to the height at which these blobs can be expected to exist, for his observations indicate that an air mass subtends an angle of about  $1^\circ$  at the observer, and that at a separation of 55 m simultaneous image-motion observations of the same object show no correlation.

Thus, the maximum height up to which the turbulence would be expected to occur is about 3000 m, and the maximum blob size is about 55 m.

Substituting these values into equation (2) together with the observed image-motion value of  $\sigma_\psi = 0.3$  arcsec gives  $\sigma_T = 0.4$  C, with a period of the order of 1 min. Such fluctuations would again not be unreasonable to expect.

Substitution of the above values for  $h$  and  $r_0$  into the expression for the range fluctuations, and use of the refractive index anomalies suggested in Table 4, means that the magnitude of  $\sigma_r$  is only of the order

$$\sigma_r = 1.34 \times 10^{5/2} \times 2 \times 10^{-8} = 8.2 \times 10^{-6} \text{ cm} .$$

## 6. CONCLUSIONS

From theoretical and heuristic considerations, the rapid-image motion has been formulated as

$$\sigma_{\psi}'' = \frac{1.45 (r_0 h)^{1/2} \sec^n z}{D^m} \left(\frac{r_0}{V}\right)^{1/2} (K - \ln \Delta T)^P \sigma_T \quad ,$$

while the experimental formulation leads to the expression

$$\sigma_{\psi}'' = 4.5 \frac{\sec^{1/2} z}{D^{1/2}} (1 - 0.38 \log \Delta t) \quad .$$

The experimental data also lead to a postulation of an eddy size of about 20 cm, which would be expected to be confined to the first 100 m of the atmosphere. The above two models are compatible if temperature fluctuations of the order of 0.01° C with periods of small fractions of seconds can be expected.

Wandering can be expressed theoretically by

$$\sigma_{\psi}'' = 0.145 \left(\frac{s}{r_0}\right)^{1/2} \sigma_T \quad ,$$

and the experimental data lead to

$$\sigma_{\psi}'' = 0.3 \quad .$$

The air masses causing the wandering appear to have a size of the order of approximately 50 m and could occur up to heights of 3 km. The period of this slow oscillatory motion is of the order of 1 min. The experimental and theoretical formulations are in agreement if slow temperature variations of about 0.4° C can be assumed to exist at heights up to 3 km.

It must be remembered that the experimental data are limited and varied, and that it is not always certain as to what region of turbulence the results refer to, or indeed that the measured quantities are not the result of some other phenomenon, and the above conclusion must be taken with caution. The fact, however, that the motion, as specified above, can be postulated without any outlandish assumptions of the air turbulence being required, as well as the fact that there are no obviously gross discrepancies between the different investigators is comforting. Certainly the conclusion can be made that, even for large-aperture cameras, image motion exists and can be significant. For example, observations with the Baker-Nunn camera of a flashing satellite can be expected to have an average image motion of about 0.7 arcsec. For the 200 mm aperture K-50 camera, the average image motion will be about 1.2 arcsec for a flashing satellite.

Brown (1960) has also deduced a formulation of image motion, which for "very short exposures" is given by

$$\sigma_{\psi}'' = \frac{k'}{D} \sec^{1/2} z \quad 1.0 < k' < 6.0 \quad .$$

This function, for average seeing conditions of  $k' = 3.5$  and  $\sec^{1/2} z = 1$ , is evaluated in Figure 3 and indicates that Brown's estimates are considerably more optimistic than are those derived here. For example, his expression applied to the Baker-Nunn camera and a flashing satellite gives an average motion of only about 0.1 arcsec and a maximum of 0.2 arcsec, and for the K-50, the average image motion according to Brown's expression is about 0.3 arcsec.

Further controlled experiments of image-motion observations are obviously required. During such observations, measurements of the rapid temperature variations as well as of wind velocity would be of value. More experience concerning the relationship of image motion with site and meteorological conditions will also be welcomed.

The observational technique of Couder, coupled with a fast shutter, is probably one of the best methods, as it removes the errors that could be contributed by instrumental vibrations. The method, however, is limited to rather small apertures because of the necessity of having two or more apertures, separated by distances greater than the air-mass size, placed in front of the objective. An alternative method, suitable for larger apertures, has been suggested by Meinel (1960) and is illustrated in Figure 4. The Baker-Nunn camera operated in a stationary mode could also be used to provide further observational data.

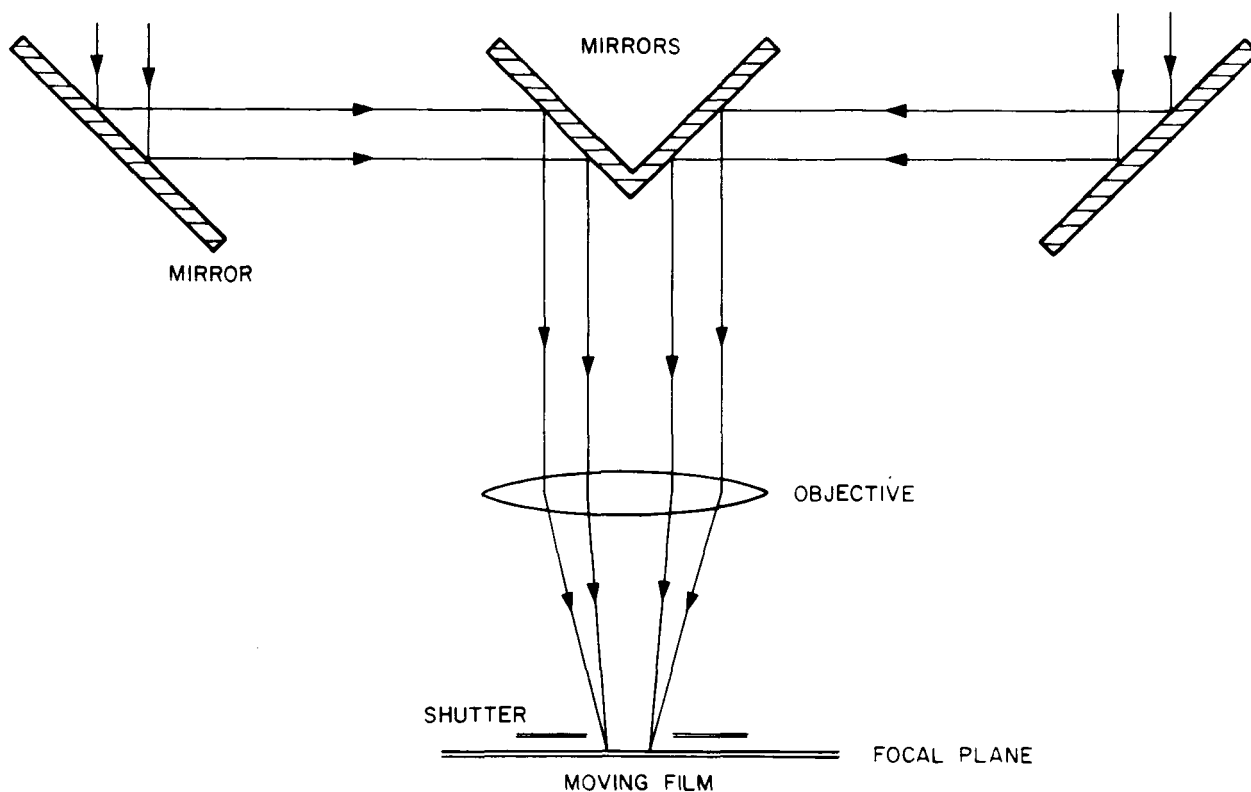


Figure 4. Possible method for observing image motion. The center mirrors deviate slightly from  $45^\circ$  to form the two separated images. The film moves in a direction at right angles to the line joining the two images. The shutter chops the resulting trails into segments corresponding to the exposure interval investigated.

## REFERENCES

ABBEY, D. G. and TAVENNER, M. S.

1967. Definition of the refraction and shimmer problem affecting geodetic observations of satellites. Presented at the Conference on Recent Research on Atmospheric Refraction for Geodetic Purposes, Vienna, March.

BAROCAS, V. and WITHERS, R. M.

1948. Effect of atmospheric variations on a stellar beam. *Observatory*, vol. 68, pp. 153-154.

BOUTET, R.

1950. Sondage optique de l'atmosphère par mesure de la scintillation. *Ann. Géophys.*, vol. 6, pp. 322-330.

BROWN, D. C.

1960. Results in geodetic photogrammetry, II. RCA Data Processing Tech. Rep. No. 65.

CHANDRASEKHAR, S.

1952. A statistical basis for the theory of stellar scintillation. *Mon. Not. Roy. Astron. Soc.*, vol. 112, pp. 475-483.

COUDER, A.

1936. Mesure photographique de l'agitation atmosphérique des images stellaires. *Comptes Rendus*, vol. 203, pp. 609-611.

HANSSON, N., KRISTENSEN, H., NETTLEBLAD, F. and REIZ, A.

1950. On the atmospheric unsteadiness. *Ann. d'Astrophys.*, vol. 13, pp. 275-279.

HOSFIELD, R.

1954. Comparisons of stellar scintillation with image motion. *Journ. Opt. Soc. Amer.*, vol. 44, pp. 284-288.

HUDSON, C. J.

1929. Irregularities in refraction. *Publ. Allegheny Obs., Univ. of Pittsburgh*, vol. 6, no. 1.

HYNEK, A.

1963. On the effects of image motion on the accuracy of measurements of a flashing satellite. *Smithsonian Contr. to Astrophys.*, vol. 6, pp. 73-75.

LAND, G.

1954. Anomalies in atmospheric refraction. *Astron. Journ.*, vol. 59, pp. 19-26.

MEGAW, E. C. S.

1954. Interpretation of stellar scintillation. *Quart. Journ. Roy. Met. Soc.*, vol. 82, pp. 231-232.

MEINEL, A. B.

1960. Astronomical seeing and observatory site selection. In *Telescopes*, edited by G. P. Kuiper and B. M. Middlehurst, pp. 154-175, Univ. of Chicago Press, Chicago.

MENZEL, D. H.

1962. Theory of atmospheric seeing. In *Proceedings, Symposium on Solar Seeing*, Rome, pp. 25-30.

MEYER-ARENDRT, J. R. and EMMANUEL, C. B.

1965. Optical scintillation; a survey of the literature. *Nat. Bur. Standards Tech. Note*, No. 225, 140 pp.

NETTLEBLAD, E.

1953. Studies of astronomical scintillation. *Meddelande Lunds Obs.*, Ser. II, No. 130, pp. 2-98.

RÖSCH, J.

1957. Sur la selection dans le temps des images telescopiques les mieux définies. *Comptes Rendus*, vol. 244, pp. 3027-3030.
- 1958a. Variations de la scintillation, de l'agitation et de l'etalement de l'image d'une étoile en fonction du diamètre de l'objectif utilisé. *Comptes Rendus*, vol. 246, pp. 384-385.
- 1958b. Etude expérimentale des défauts de l'image d'une étoile en fonction du diamètre de l'objectif utilisé. *Comptes Rendus*, vol. 246, pp. 559-561.

SCHLESINGER, F.

1916. Irregularities in atmospheric refraction. Publ. Allegheny Obs.,  
Univ. of Pittsburgh, vol. 3, no. 1.

SCHMID, H. H.

1965. Precision and accuracy considerations for the execution of geo-  
metric satellite triangulation. Presented at the 2nd International  
Symposium on the Uses of Artificial Satellites for Geodesy,  
Athens, April.



## BIOGRAPHICAL NOTE

KURT LAMBECK graduated in geodesy from the University of New South Wales, Australia, in 1963. He studied at the Geodetic Institute, Delft, Holland, in 1964 and at the National Technical University of Athens in 1965. He also studied at the Department of Surveying and Geodesy, Oxford University, England, and was Consultant Geodesist with the Smithsonian Astrophysical Observatory during the summer of 1966.

Dr. Lambeck received his D. Phil. in geodesy from Oxford in 1967. He joined SAO in the same year and is currently working as a geodesist.

## NOTICE

This series of Special Reports was instituted under the supervision of Dr. F. L. Whipple, Director of the Astrophysical Observatory of the Smithsonian Institution, shortly after the launching of the first artificial earth satellite on October 4, 1957. Contributions come from the Staff of the Observatory.

First issued to ensure the immediate dissemination of data for satellite tracking, the reports have continued to provide a rapid distribution of catalogs of satellite observations, orbital information, and preliminary results of data analyses prior to formal publication in the appropriate journals. The Reports are also used extensively for the rapid publication of preliminary or special results in other fields of astrophysics.

The Reports are regularly distributed to all institutions participating in the U. S. space research program and to individual scientists who request them from the Publications Division, Distribution Section, Smithsonian Astrophysical Observatory, Cambridge, Massachusetts 02138.